Hindawi
International Journal of Rotating Machinery
Volume 2020, Article ID 8867416, 11 pages
https://doi.org/10.1155/2020/8867416

Research Article

Utilization of Open-Source OpenFOAM Code to Examine the Hydrodynamic Characteristics of a Linear Jet Propulsion System with or without Stator in Bollard Pull Condition

Parviz Ghadimi, Negin Donyavizadeh, and Pouria Taghikhani

Department of Maritime Engineering, Amirkabir University of Technology, Tehran, Iran

Correspondence should be addressed to Parviz Ghadimi; pghadimi@aut.ac.ir

Received 25 May 2020; Revised 8 November 2020; Accepted 17 November 2020; Published 9 December 2020

Academic Editor: Cheng Xu

With the development of high-speed crafts, new propulsion systems are introduced into the marine industry. One of the new propulsion systems is linear jet which is similar to pump jet and has a rotor, a stator, and a duct. The main difference between this system and pump jet is the placement of linear jet system under the hull body and inside a tunnel. Since this system, like a water jet, is inside the tunnel, the design idea of this system is a combination of a water jet and pump jet. In this paper, hydrodynamic performance of linear jet propulsion system is numerically investigated. To this end, the OpenFOAM software is utilized and RANS steady equations are solved using a k-ε turbulent model. The linear jet geometry is produced by assembling a Kaplan rotor, stator with a NACA 5505 cross section, and a decelerating duct. The results of numerical solution in the form of thrust, torque coefficient, and efficiency are compared with available experimental data for a ducted propeller, and good agreement is displayed. Subsequently, the hydrodynamic parameters are computed in two conditions: with a stator and without a stator. By comparing the results, it is observed that the total thrust coefficient of the propulsion system with a stator at all advance ratios increases by at least 40%. It is further observed that addition of a stator also improves its efficiency.

1. Introduction

Linear jet propulsion system is one of the new propulsion systems in the marine industry. To upgrade the ducted propulsion and pump-jet systems, the linear jet propulsion system was introduced by a researcher in 2012. Sorbello [1] showed that the linear jet system can increase the Bollard force by about 50% without increasing the required engine power. Overall, this system can be used for vessels with 20 to 60 m length. The applicational range of speed in this system is between 25 and 40 knots. This system is like a ducted propeller system and includes a rotor and a duct. However, the difference between this system and the ducted propeller is the presence of a fixed stator which is connected to the duct. The stator can be placed upstream or downstream of the rotor. The presence of the stator causes the conversion of the rotational speed of the rotor to an axial speed behind the rotor. The outlet flow of the rotor also becomes uniform by a duct [2]. Considering the long history of the use of ducted propellers in varieties of boats and ships, different experimental and numerical works have been conducted in this regard. One of these works is the experiment performed by Oosterveld [3] on a propeller of ka 4-70 with a duct of 19A. Their results have been used for validation of many numerical investigations. He presented the open-water test results of the ducted propeller systems which are suitable for push boats and tugs. Several years later, Taketani et al. [4] placed a Kaplan propeller series inside a 19A duct and examined the flow around the propeller. Nevertheless, their results showed a higher bollard pull performance than the conventional propeller. Subsequently, Baltazar et al. [5] and Bosschers and van der Veeken [6] made changes to the 19A duct to improve the wake generated by the vessels. The analysis was carried out for the propeller ka 4-70 operating in two conditions: without a modified 19A duct and with a modified 19A duct. Later, Yongle et al. [7] examined

Table 1: Geometric specifications for ducted propeller ka 4-70 [3].

Characteristic	Duct	Propeller section	Z	$D_{propeller}$	P/D	AOA	$D_{hub}/D_{propeller}$
Value	19A	Kaplan	4	0.2	1	0.7	0.2

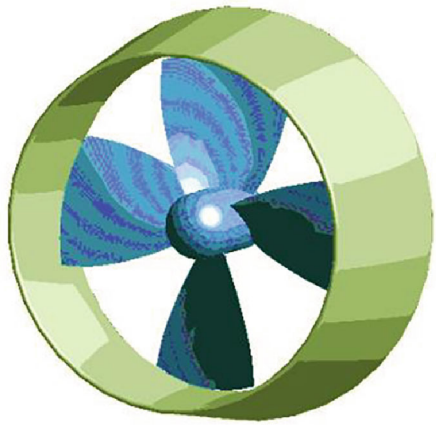

Figure 1: Three-dimensional model of the ducted propeller.

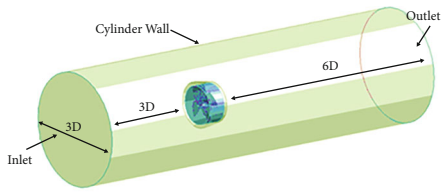

Figure 2: Dimensions of the computational domain with determination of the boundary conditions.

Table 2: Experimental results for validation [3].

Advance ratio	Thrust coefficient	Torque coefficient
0.2	0.416394	0.0423
0.4	0.311192	0.0389
0.6	0.184658	0.0315
0.8	0.0310027	0.0193

Table 3: Boundary conditions.

Boundary	Type of boundary condition
Inlet	Velocity inlet
Outlet	Pressure gradient
Propeller & hub	No-slip wall
Duct	No-slip wall
Cylindrical wall	Free-slip wall

the effects of changes of tip clearance. Simulation results showed that the tip loss slope was not linear at high advance ratio due to the reversed pressure at the leading edge. In the same year, Valčić and Dejhalla [8] estimated the open-water characteristics of the four-blade ka 4-70 propeller with the duct of 19A.

Along with the development of a ducted propeller system, another system called a pump jet was formed. The difference between this system and the ducted propeller system was the presence of stator blades after the propeller. The presence of these blades causes the output flow [9]. However, this idea has been used for many years only on submarine and the first model was used in the British submarines in 1996 [10]. In 2009, Kim [11] solved the numerical solution of the pump jet using the OpenFOAM software and examined the turbulence flow around a pump jet. Suryanarayana et al. [12] also performed experiments on a symmetrical body with a pump-jet propulsion system. According to their tests, the propulsion system of the pump jet has a wider range of performance than the ducted propeller, but the efficiency of this pump jet does not exceed 40%. In 2013, Lü et al. [13] examined the flow through a pump jet by solving the Navier-Stokes equation using the turbulence model SST k-ω. It was shown that a decrease in the distance between the pods and the hull leads to an increase in the efficiency of the pods and the thrust coefficient. In addition, Pan et al. [14] performed similar simulations in the same year with the turbulence model k-ω SST in a finite volume scheme and examined vortex tips. Another numerical analysis in the field of pump jet focusing on the occurrence of cavitation was conducted by Shi et al. [15]. The effects of different advance ratios, cavitation number, and flow velocity on cavitation characteristics of the pump jet were studied. As a result, it was observed that, when the cavitation occurs on the blades, the propeller thrust and torque decrease significantly, thereby causing a 15% reduction in open-water efficiency. In 2016, Motallebi-Nejad et al. [16] performed numerical analysis of the pump-jet system using the periodic domain. To validate their results, they placed a Kaplan 4-70 propeller, produced by PropCad software into a 19A duct and analyzed it using Ansys-CFX software. Pan et al. [17] also conducted a numerical analysis of the pump-jet thrust system. This numerical study was based on the unsteady Reynolds-averaged Navier-Stokes computational fluid dynamics method. Their numerical simulations accurately predicted the propulsion efficiency changes and the cavitation inception and extension on the suction side of the rotor blades. Moreover, Lu et al. [18, 19] investigated tip clearance effects on the performance of the pump-jet propulsion. Results showed that the structure and characteristics of the tip leakage vortex and the efficiency of the propulsion reduced with an increase in the tip clearance size. One of the most recent studies, which directly refer to the linear jet propulsion system, was conducted in 2020 by Donyavizadeh and Ghadimi [20]. They numerically examined the thickness and length of the camber in the stator, which is one of the main components of the linear jet propulsion system.

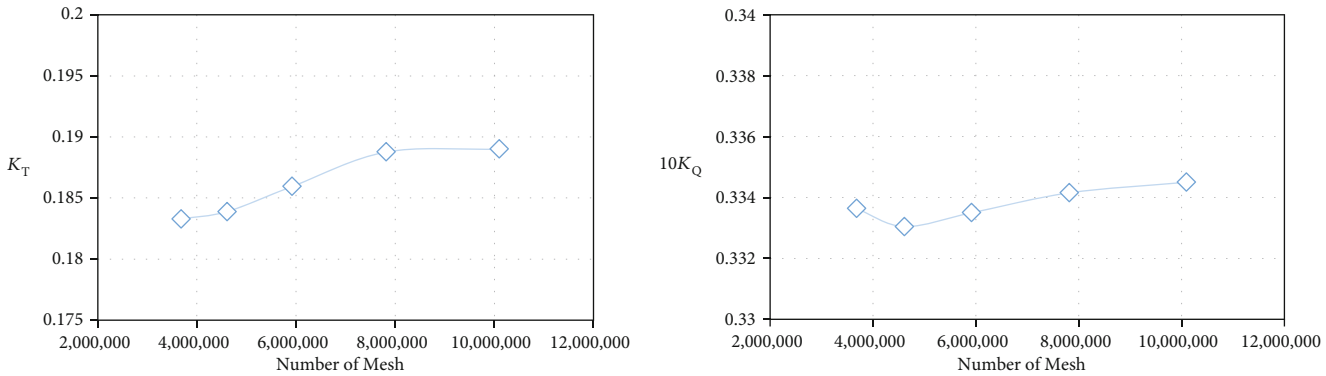

Figure 3: Thrust and torque coefficients in $J = 0.6$ for different numbers of elements.

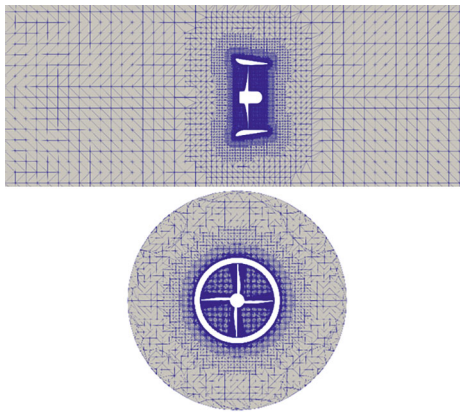

Figure 4: An overview of the computational grid used in numerical solving.

In the present study, considering the importance of stator on the performance of the linear jet propulsion system and the lack of any data in the field of linear jet ropulsion system, the effect of the presence of stator in a linear jet propulsion system is examined. The presence of stator blades causes the output flow and increases the resistance of the ship, but it improves the wake of vessels, thereby increasing the final efficiency of the propulsion system. Numerical simulations are conducted solving RANS equations. The OpenFOAM software is used to perform the simulations. Geometry of cross section of the rotor is selected from Kaplan series, while the cross section of a duct is NACA 0010. The computational domain is a cylinder, and mesh type is unstructured. For this domain, the mesh sensitivity is checked, and the optimum mesh size is selected for a solution with high accuracy. For numerical accuracy verification, a ducted propeller from Kaplan series is analyzed in OpenFOAM software. Subsequently, the geometry of the linear jet propulsion system is examined with the stator. Two different case studies are considered; one with stator and another with no stator, and they are numerically analyzed. For both studies, the results are expressed in terms of thrust and torque at different advance ratios.

Table 4: Comparison of numerical data with experimental data [3].

J	K_T (NUM)	K_T (EXP)	Percent error in K_T	K_Q (NUM)	K_Q (EXP)	Percent error in K_Q
0.2	0.4175	0.4163	0.28	0.0433	0.0423	2.36
0.4	0.3016	0.3111	3.05	0.0403	0.0389	3.59
0.6	0.1857	0.1846	0.59	0.0333	0.0315	5.71
0.8	-0.0331	0.0310	6.77	0.0179	0.0193	7.25

2. Governing Equations

For analyzing the flow around ducted propeller, continuity and momentum equations are solved. The flow condition is assumed to be incompressible. The conservation of mass and momentum is solved with three-dimensional RANS equations given in Equations (1) and (2).

$$\frac{\partial}{\partial x_i}(\rho \bar{u}_i) = 0, \tag{1}$$

$$\frac{\partial \rho}{\partial t}(\rho \bar{u}_i) + \frac{\partial \rho}{\partial x_j}(\rho \bar{u}_i \bar{u}_j) = \rho \bar{F}_i - \frac{\partial \bar{p}}{\partial x_i} + \frac{\partial}{\partial x_j}\left[\mu\left(\frac{\partial \bar{u}_i}{\partial x_j} + \frac{\partial \bar{u}_j}{\partial x_i}\right)\right]. \tag{2}$$

For computing the thrust and torque of the propeller, nondimensional coefficients such as advance ratio (J), thrust coefficient (K_T), torque coefficient (K_Q), and efficiency (η_O) are used which are seen in Equations (3) to (6):

$$J = \frac{V_A}{n \cdot D}, \tag{3}$$

in which, V_A is advance velocity of the water into the propeller.

$$K_T = \frac{T}{\rho \cdot n^2 \cdot D^4}, \tag{4}$$

$$K_Q = \frac{Q}{\rho \cdot n^2 \cdot D^5}. \tag{5}$$

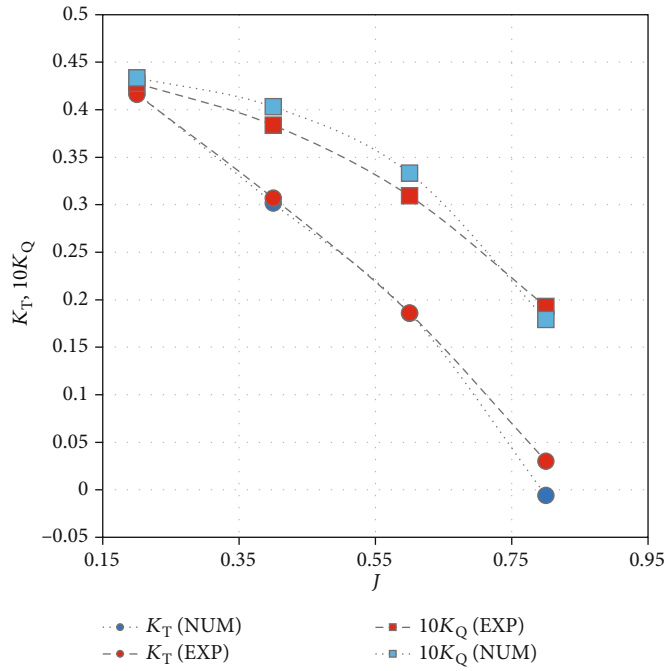

Figure 5: Comparison of numerical and experimental results [3] for thrust and torque coefficients.

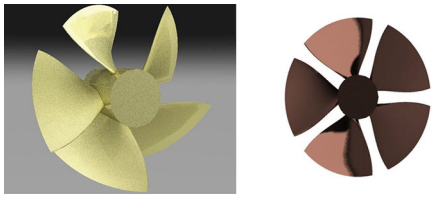

Figure 6: Schematics of the rotor blade produced in PropCad.

Table 5: General information of the rotor blade.

Number of blades:	5
Diameter	185
Pitch	1.2
Rake	0
Skew angle	3.1

Table 6: Information of decelerating duct section.

NACA 0010 Airfoil $M = 0.0\%$, $P = 0.0\%$, $T = 10.0\%$
Chord (mm): 100
Radius (mm): 0
Thickness (%): 100
Origin (%): 0
Pitch (degree): 0

Equation (6) is used to calculate the propeller efficiency in an open-water condition:

$$\eta_O = \frac{J}{2\pi}\frac{K_T}{K_Q}, \tag{6}$$

where ρ is the fluid density around the propeller, n is the rotational speed of the propeller, and D is diameter of the propeller.

In this study, OpenFOAM software is used to solve numerical problems. The flow simulation is based on the solution of the RANS equations. The k-ε method is used for modeling of the turbulence effect. The algorithm intended for the iteration method is also PIMPLE [21]. This algorithm is specific to OpenFOAM software, and it is a combination of SIMPLE and PISO algorithms [22]. Based on the guidelines specified by OpenFOAM software developers, two solvers are proposed to solve the propeller issue. From these two, one solves for the flow around the propeller with the presence of cavitation and the other with no cavitation. Since the aim of the current study is not to study cavitation, a PimpleDyMFoam solver is selected, which can model the noncavitation case.

3. Validation of Numerical Method

For verifying the numerical solution, available experimental results [3] for a ducted propeller are utilized. For this purpose, a ducted propeller is used as a simplified case of a linear jet system, and its specifications are given in Table 1. The three-dimensional model of the ducted propeller is shown in Figure 1.

The computational domain is considered two cylinders (Figure 2). The small cylinder is around the propeller and

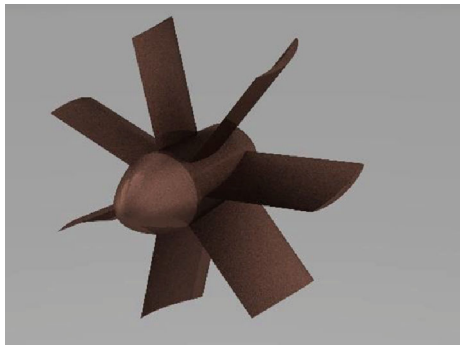

Figure 7: Stator image produced with a NACA 5505 cross section.

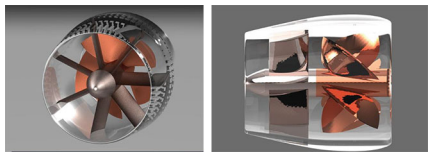

Figure 8: Three-dimensional geometry of the linear jet propulsion system.

Table 7: Thrust force calculated for the linear jet system with a stator.

J	Pressure thrust for rotor	Viscous thrust for rotor	Pressure thrust for duct & stator	Viscous thrust for duct & stator	Total thrust	K_T
0	292.391	-2.5106	34.3901	-0.749	323.52124	1.37154
0.2	246.086	-3.2313	40.9112	-2.055	281.71124	1.19429
1.1	199.053	-3.7106	8.00042	-11.22	192.12737	0.81451
2	192.865	-4.2118	-67.949	-23.26	97.44924	0.41313
3	107.457	-5.6565	-143.23	-44.31	-85.74476	-0.3635

has a rotational motion. This cylinder is inside a larger cylinder. This is the convenient way for modeling the rotation of the propeller.

The hydrodynamic characteristics of the experimental test for the ducted propeller are given in Table 2.

In Table 2, the computed thrust and torque coefficients at various advance ratios in the range 0.2 to 0.8 are shown. Based on the presented results, the thrust and torque coefficients are reduced with an increase in advance ratios.

To perform numerical calculations, the initial and boundary conditions of the problem must be determined, which are shown in Table 3.

As shown in Figure 2 and Table 3, the free-slip wall boundary condition is applied on the cylindrical walls. At the start of the computational domain, the applied input boundary condition is flow with a constant speed (1 m/s) toward the propeller. To establish the mass conservation equation, zero pressure gradient is applied as boundary condition at the end of the computational domain. However, the propeller and part of the shaft are placed inside a rotating cylinder, to apply a moving mesh.

Table 8: Torque force calculated for the linear jet system with a stator.

J	Pressure torque for rotor	Viscous torque for rotor	Torque	K_Q	$10*K_Q$
0	26.187	0.1361	26.32	0.62	6.1996
0.2	21.979	0.1539	22.13	0.521	5.2128
1.1	19.528	0.1488	19.68	0.463	4.6343
2	18.573	0.1692	18.74	0.441	4.4142
3	10.895	0.2287	11.12	0.262	2.6199

To achieve better accuracy in numerical solution, it is essential to check the quality and size of the mesh elements generated in the computational domain. Mesh grid in the computational domain is generated by the SnappyHexMesh tool in open-source OpenFOAM software. The results of this study for the thrust force are shown in Figure 3.

The number of elements in the domain is about 8 million. As evident in Figure 3, with an increase in the number of elements (more than 6 million), there is no change in thrust and torque coefficients. Figure 4 shows the generated elements around the duct and the propeller.

Results of computation in the form of thrust coefficient and torque coefficient are displayed in Table 4. The obtained numerical results are compared with experimental data [3].

Based on the presented results, it can be concluded that the average of errors is less than 3%. The computed thrust and torque coefficients are also displayed in Figure 5.

As observed in Figure 5, good compliance is achieved between numerical results and experimental data [3] for the thrust and torque coefficients.

4. Results and Discussion

To investigate the effects of the presence of a stator on the performance of a linear jet propulsion system, the linear jet system is generated with the following characteristics. Three parts of this system are separately produced and eventually assembled.

4.1. Geometry of Linear Jet System. The PropCad software has been used to produce the rotor blades of the system which has 5 blades. Its section is selected from Kaplan series (Figure 6). The overall data for this blade is also shown in Table 5.

To generate a duct, a decelerating type is used. For this purpose, a NACA 0010 foil section is utilized. Its specification is illustrated in Table 6.

In this design, a stator with 7 blades and a NACA 5505 cross section is selected, as shown in Figure 7.

Finally, after assembling the produced parts, which includes a stator, a duct and a rotor, a linear jet propulsion system is generated. A three-dimensional geometry of this system is displayed in Figure 8.

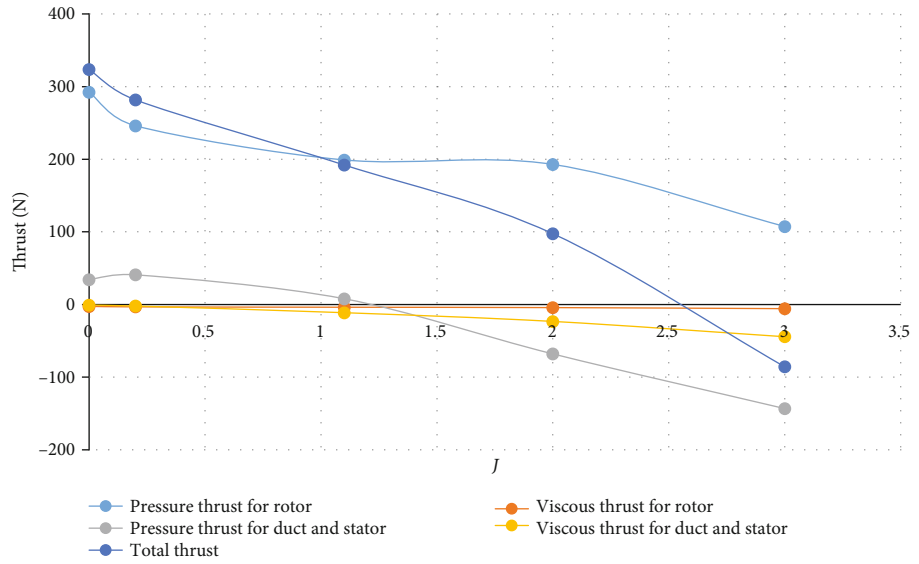

Figure 9: Thrust force calculated for the linear jet system with a stator.

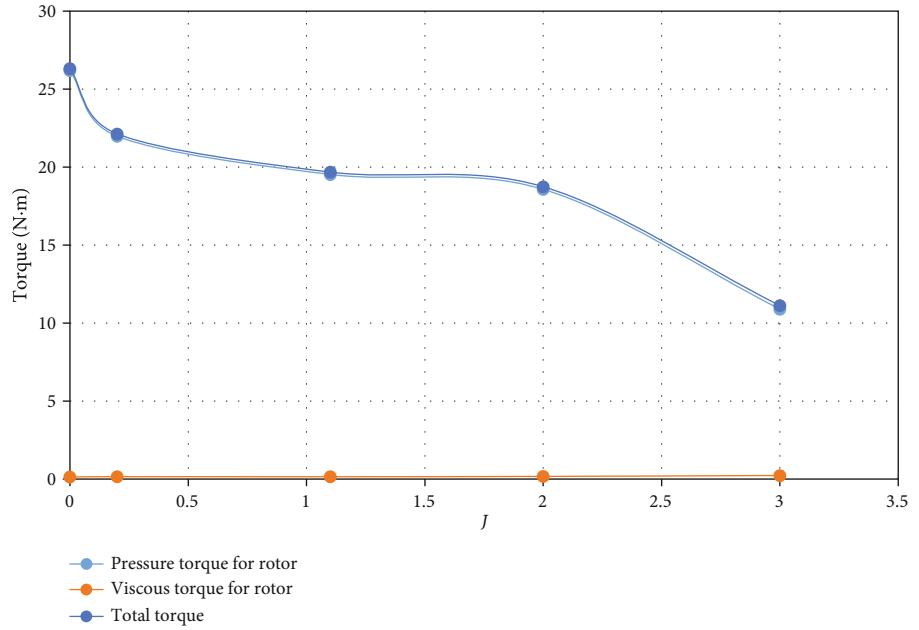

Figure 10: Torque force calculated for the linear jet system with a stator.

Table 9: Thrust force calculated for the linear jet system without a stator.

J	Pressure thrust for rotor	Viscous thrust for rotor	Pressure thrust for duct & stator	Viscous thrust for duct & stator	Total thrust	K_T
0	263.002	-1.0077	-33.178	2.0571	230.87	0.97877
0.2	240.305	-1.477	-34.239	0.34076	204.93	0.86878
1.1	218.923	-3.1282	-61.993	-8.7453	145.06	0.61496
2	177.943	-4.6833	-100.7	-20.234	52.328	0.22184
2.5	118.804	-5.4916	-126.59	-28.403	-41.68	-0.1767

Table 10: Torque force calculated for the linear jet system without a stator.

J	Pressure torque for rotor	Viscous torque for rotor	Torque	K_Q	$10*K_Q$
0	24.098	0.0916	24.19	0.5697	5.6971
0.2	22.328	0.1028	22.43	0.5283	5.283
1.1	21.011	0.138	21.15	0.4981	4.9811
2	17.196	0.1805	17.38	0.4093	4.0925
2.5	11.842	0.2052	12.05	0.2837	2.8374

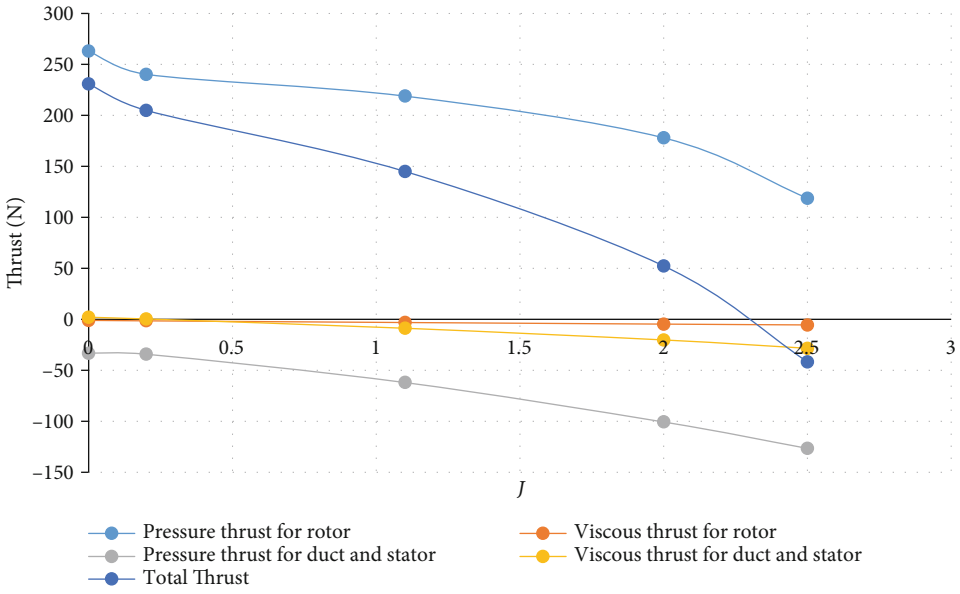

Figure 11: Thrust force calculated for the linear jet system without a stator.

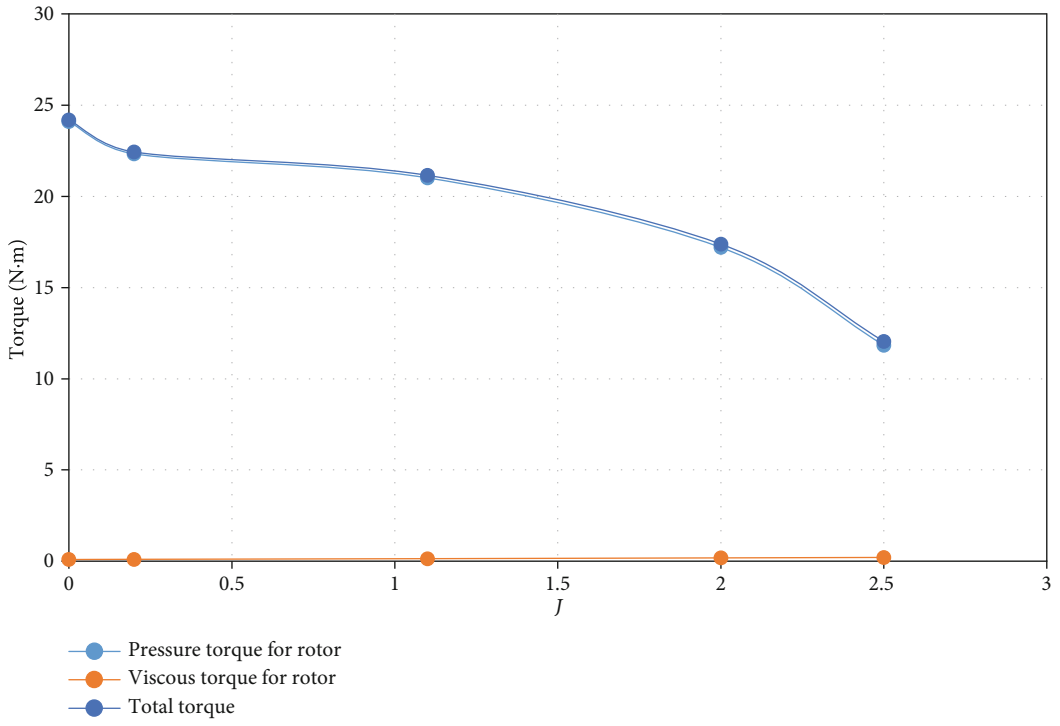

Figure 12: Torque force calculated for the linear jet system without a stator.

4.2. Hydrodynamic Characteristics of Linear Jet System with and without a Stator. Five simulations are carried out in an open-water condition in the presence and absence of a stator, and hydrodynamic characteristics are fully realized. The numerical results obtained for thrust, torque, and efficiency with the presence of a stator are presented in Tables 7 and 8. The thrust and torque for the linear jet system are calculated separately for the components of the system such as rotor, stator, and duct. For better understanding, these results are presented in Figure 9.

As evident in Table 7 and Figure 9, the rotor always produces a thrust force for the vessel. However, the duct segment starts to produce a negative pressure thrust from the advance ratio of 1.2 which is also compatible with the nature of the ducts. In the last row of Table 7, the negative thrust of the duct and the stator is much more than the

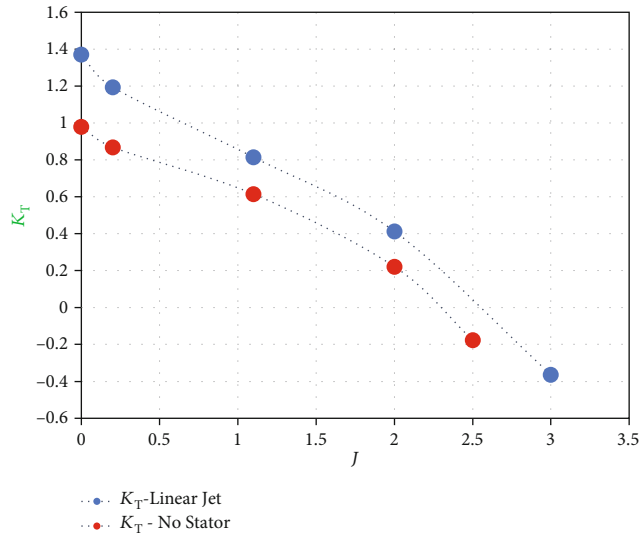

(a)

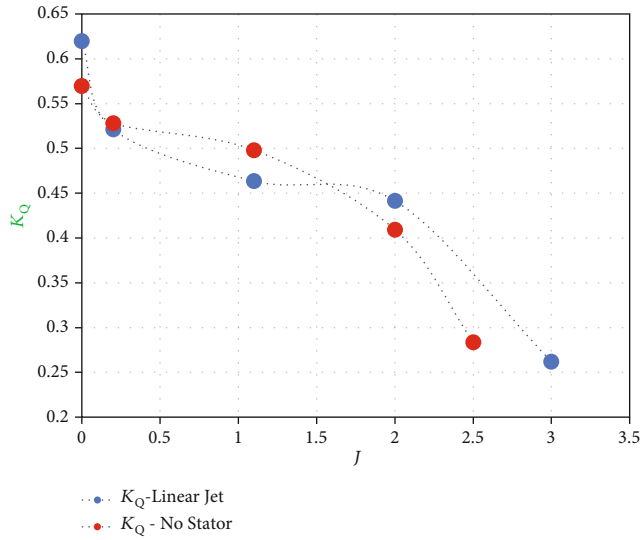

(b)

Figure 13: Comparison of forces in the presence and absence of a stator: (a) thrust coefficient; (b) torque coefficient.

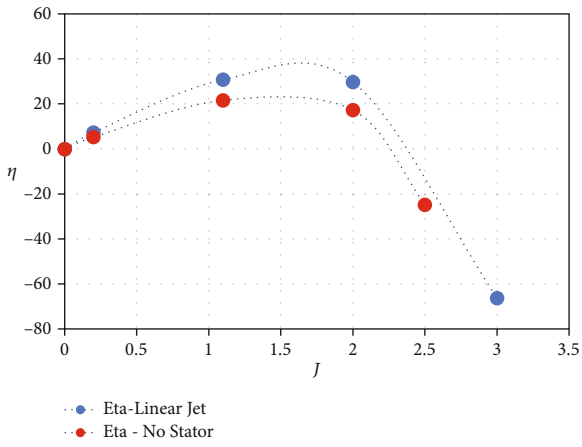

Figure 14: Comparison of efficiency in the presence and absence of a stator.

Table 11: Rotor rotational speed values to investigate a bollard pull power.

n (rps)	n (rpm)	n (rad/s)
1.00	60.00	6.283185307
10.00	600.00	62.83185307
15.00	900.00	94.24777961

rotor thrust, so the total thrust is negative. It can be estimated by interpolation that from the advanced ratio of 2.4 on this system does not have the required performance. It should be noted that this is a large number for a ducted propeller performance.

The computed torque forces are illustrated in Table 8 and Figure 10.

Table 12: Thrust force calculated for the linear jet system in bollard pull mode.

Type of system	n (rpm)	Pressure thrust for rotor	Viscous thrust for rotor	Pressure thrust for duct & stator	Viscous thrust for duct & stator	Total thrust	K_T
Without stator	60	3.1468	-0.028	-0.3782	0.0151	2.7557	2.6285789
	600	115.54	-0.5095	-15.258	0.9147	100.68	0.9603763
	900	263	-1.0077	-33.178	2.0571	230.87	0.9787682
With stator	60	3.1444	-0.0277	-0.4431	0.0016	2.6753	2.5518888
	600	135.02	-0.7668	14.5523	0.3011	149.11	1.4223175
	900	292.39	-2.5106	34.3901	-0.749	323.52	1.3715393

Based on Table 8, unlike the thrust force, torque force decreases with an increasing advance ratio but shows a positive value. To assess the effect of a stator on hydrodynamic characteristics of the stator, the calculation is repeated for the linear jet system without a stator. Results are shown in Tables 9 and 10. For better understanding, these results are presented in Figures 11 and 12.

By comparing the results in Tables 7 and 9, it is observed that the presence of a stator has a positive effect on the rotor's thrust force. However, in the absence of a stator, the duct thrust force is always negative and this is consistent with the nature of the duct. When the advanced ratio is zero, the thrust coefficient in the presence of a stator is about 40% higher than the nonstator condition.

The results of torque force in the case of the system with a stator are displayed in Table 10.

The computed thrust and torque coefficients in the presence and absence of a stator are compared in Figure 13.

As evident in Table 10 and Figure 13, thrust coefficient increases in the presence of a stator by about 40% at low speeds and further increases by about 100% at high speeds. The presence of the stator also increases the range of thrust coefficient in this system. Therefore, it can be concluded that the presence of a stator in this system has a positive effect on the thrust force. Torque variation in the presence and absence of a stator (as shown in Figure 13) does follow a pattern, and the results cannot be conclusive. Of course, at the beginning and end of the graph corresponding to very low and very high speed, torque coefficient has increased.

To investigate the effects of a stator, the efficiency of this system in both no-stator and stator mode is illustrated in Figure 14.

It is clearly observed in Figure 14 that efficiency significantly increases in an open-water condition in the horizontal and vertical direction.

4.3. Effect of Stator on Bollard Pull in the Linear Jet Propulsion System. One of the applications of the linear jet propulsion systems is to increase bollard pull in tugboats. Meanwhile, one of the most important parameters that is measured in the bollard pull simulations is the thrust coefficient. For this purpose, flow is assumed to be at zero velocity, while the rotor is driven at different speeds and thrust coefficient at is measured at each speed [23].

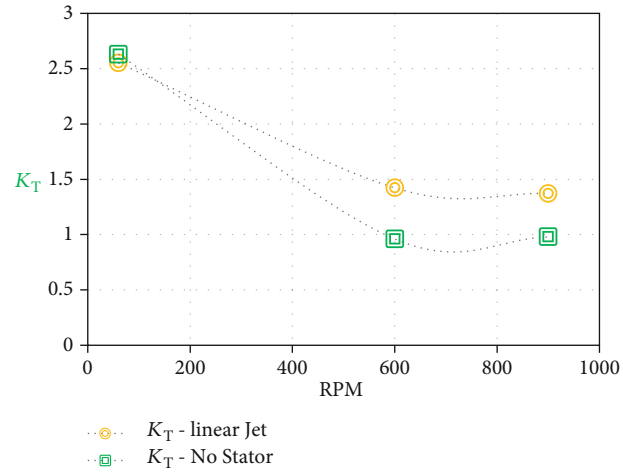

Figure 15: Comparison of thrust coefficient in bollard pull mode in the presence and absence of a stator.

This study was carried out at three different rotating speeds which are indicated in Table 11.

Thrust and torque coefficients for different rotational speeds are computed in the presence and absence of a stator. The obtained thrust coefficients for three rotor's rotational speeds are presented in Table 12.

As observed in Table 12, force variation at low rotational speed is not quite noticeable. However, up to 50% increase is seen in the thrust force at higher rotational speeds. To better illustrate these results, thrust coefficient diagram is shown in Figure 15.

Torque force is also computed, and its influence on different components of the linear jet propulsion system is analyzed. Torque force and torque coefficients for three rotor rotational speeds in the presence of a stator are presented in Table 13 and Figure 16, respectively.

It is quite evident in Table 13 and Figure 16 that torque increases slightly at high rotational speed in the presence of a stator. This can be attributed to the interaction between the stator and the rotor. Needless to say, the general trend of torque coefficient diagram is very similar to the thrust force in the presence of a stator.

Streamlines of the flow field around the linear jet are presented with the presence of a stator and without a stator in Figures 17 and 18, respectively.

Table 13: Torque force calculated for the linear jet system in bollard pull mode.

Type of system	n (rpm)	Pressure torque for rotor	Viscous torque for rotor	Torque	K_Q	$10*K_Q$
Without stator	60	0.28663	0.0021	0.289	1.52989499	15.2989
	600	10.6028	0.0443	10.65	0.56421527	5.64215
	900	24.0976	0.0916	24.19	0.56971001	5.6971
With stator	60	0.28665	0.0021	0.289	1.53001216	15.3001
	600	12.2604	0.052	12.31	0.65246798	6.52468
	900	26.1867	0.1361	26.32	0.61996261	6.19963

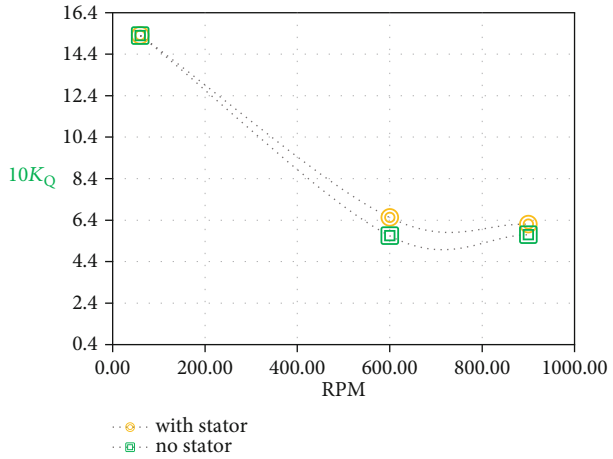

Figure 16: Comparison of torque coefficient in bollard pull mode in the presence and absence of a stator.

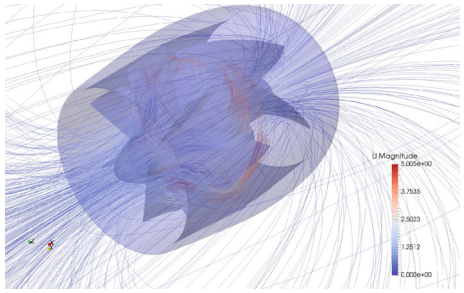

Figure 17: Streamlines in bollard pull mode in the presence of a stator at 600 rpm.

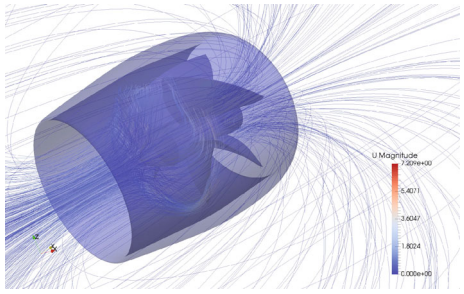

Figure 18: Streamlines in bollard pull mode in the absence of a stator at 600 rpm.

5. Conclusion

In this paper, a linear jet propulsion system which is an improved system, is numerically investigated to examine the influence of the presence and absence of a stator on its hydrodynamic performance. For numerical simulation, the OpenFOAM software is used. RANS steady equations are solved using the k-ε turbulent model. For validation purposes, the hydrodynamic characteristics of a ducted propeller including thrust coefficient and torque coefficients compared with available experimental data and good accordance are achieved.

The linear jet system model is produced by assembling a Kaplan rotor, NACA 5505 stator blades, and 19A ducts. Hydrodynamic parameters including thrust, torque, and efficiency in open-water conditions are analyzed in two cases: with a stator and with no stator. Based on the obtained results, it is seen that the presence of a stator has a positive effect on the rotor's thrust force. When the advanced ratio is zero, the thrust coefficient in the presence of a stator is about 40% higher than that in the nonstator system. Also, in this case, the torque coefficient in the presence of a stator is about 9% higher than that in the nonstator system. At different advance ratios, it is well established that in the presence of a stator, the efficiency is higher than the case without a stator. The maximum efficiency of the linear jet propulsion system occurs at an advance ratio of 1.5, which is more different than the case without a stator. Due to high importance of bollard pulling power, the torque and torque coefficients are again calculated and presented for two states of presence and absence of the stator at different rotational speeds and the bollard pull condition. It is observed that, at some rotational speeds, the thrust increases by about 100%. The presence of a stator in this case adds a significant thrust force to the system and improves its efficiency.

Future studies may include an extensive parametric study to obtain duct geometric characteristics such as optimal length. Seeking the suitable propeller shape for obtaining optimal parameters such as pitch is also another task that needs to be pursued.

Data Availability

Data is available upon request from the corresponding author.

Conflicts of Interest

The authors declare that there is no conflict of interest.

References

[1] K. S. Sorbello, "The Voith Linear Jet: combining the best of two options," 2012, https://gcaptain.com/voith-linear-jet-combining-options/.

[2] J. S. Carlton, *Marine Propulsion and Propellers.*, Butterworth Heinemann, London, UK, 3rd edition, 2012.

[3] M. W. C. Oosterveld, *Ducted propeller characteristics*, In RINA symposium on ducted propellers, 1973.

[4] T. Taketani, K. Kimura, N. Ishii, M. Matsuura, and Y. Tamura, "Advanced design of a ducted propeller with high bollard pull performance," *RN*, vol. 6, p. 105, 2009.

[5] J. Baltazar, J. A. C. Falcão de Campos, and J. Bosschers, "Open-water thrust and torque predictions of a ducted propeller system with a panel method," *International Journal of Rotating Machinery*, vol. 2012, Article ID 474785, 11 pages, 2012.

[6] J. Bosschers and R. van der Veeken, *Open water tests for propeller Ka4-70 and duct 19A with a sharp trailing edge*, MARIN Report, (224457-2-VT), 2008.

[7] D. Yongle, S. Baowei, and W. Peng, "Numerical investigation of tip clearance effects on the performance of ducted propeller," *International journal of naval architecture and ocean engineering*, vol. 7, no. 5, pp. 795–804, 2015.

[8] M. Valčić and R. Dejhalla, "Neural network prediction of open water characteristics of ducted propeller," *Pomorski zbornik*, vol. 49, no. 1, pp. 101–115, 2015.

[9] FathomShipping, *Propeller technology to make your ship more efficient*, 2012, https://gcaptain.com/propeller-technology-ship-efficient/.

[10] P. L. Vosper and A. J. Brown, "Pumpjet propulsion-a British splendid achievement," *J. Naval Engineering*, vol. 36, no. 2, 1996.

[11] S. E. Kim, "Multiphase CFD simulation of turbulent cavitating flows in and around marine propulsors," *In Proceedings of Open Source CFD International Conference*, pp. , 200912-13, 2009.

[12] C. Suryanarayana, B. Satyanarayana, and K. Ramji, "Performance evaluation of an underwater body and pumpjet by model testing in cavitation tunnel," *International Journal of Naval Architecture and Ocean Engineering*, vol. 2, no. 2, pp. 57–67, 2010.

[13] X.-j. Lü, Q.-d. Zhou, and B. Fang, "Hydrodynamic performance of distributed pump-jet propulsion system for underwater vehicle," *Journal of Hydrodynamics*, vol. 26, no. 4, pp. 523–530, 2014.

[14] G. Pan, B. Hu, P. Wang, Z. D. Yang, and Y. Y. Wang, "Numerical simulation of steady hydrodynamic performance of a pump-jet propulsor," *Journal of Shanghai Jiaotong University*, vol. 47, no. 6, pp. 932–937, 2013.

[15] Y. Shi, G. Pan, Q. Huang, and X. Du, "Numerical Simulation of Cavitation Characteristics for Pump-jet Propeller," *Journal of Physics: Conference Series*, vol. 640, no. 1, p. 012035, 2015.

[16] M. Motallebi-Nejad, M. Bakhtiari, H. Ghassemi, and M. Fadavie, "Numerical analysis of ducted propeller and pumpjet propulsion system using periodic computational domain," *Journal of Marine Science and Technology*, vol. 22, no. 3, pp. 559–573, 2017.

[17] G. Pan, L. Lu, and P. K. Sahoo, "Numerical simulation of unsteady cavitating flows of pumpjet propulsor," *Ships and Offshore Structures*, vol. 11, no. 1, pp. 64–74, 2016.

[18] L. Lu, G. Pan, J. Wei, and Y. Pan, "Numerical simulation of tip clearance impact on a pumpjet propulsor," *International journal of naval architecture and ocean engineering*, vol. 8, no. 3, pp. 219–227, 2016.

[19] L. Lu, G. Pan, and P. K. Sahoo, "CFD prediction and simulation of a pumpjet propulsor," *International Journal of Naval Architecture and Ocean Engineering*, vol. 8, no. 1, pp. 110–116, 2016.

[20] N. Donyavizadeh and P. Ghadimi, "Efficacy Analysis of Thickness and Camber Size of Cross Section of the Stator on Hydrodynamic Parameters in Linear Jet Propulsion System," *Mathematical Problems in Engineering*, vol. 2020, Article ID 5861948, 17 pages, 2020.

[21] *Open FOAM guide/The PIMPLE algorithm in Open FOAM*, 2017, Retrieved from https://openfoamwiki.net/index.php/OpenFOAM_guide/The_PIMPLE_algorithm_in_OpenFOAM.

[22] P. DyMFoam, 2014, Retrieved from https://openfoamwiki.net/index.php/PimpleDyMFoam.

[23] T. H. Joung, H. S. Choi, S. K. Jung, K. Sammut, and F. He, "Verification of CFD analysis methods for predicting the drag force and thrust power of an underwater disk robot," *International Journal of Naval Architecture and Ocean Engineering*, vol. 6, no. 2, pp. 269–281, 2014.